Available online at www.sciencedirect.com
ScienceDirect
Ceramics International 36 (2010) 333–338
CERAMICS INTERNATIONAL
www.elsevier.com/locate/ceramint

Optical properties of amorphous organo-modified silica nanoparticles produced via co-condensation method

M. Jafarzadeh [b], I.A. Rahman [a,*], C.S. Sipaut [b]

[a] School of Dental Sciences, Health Campus, Universiti Sains Malaysia, 16150 Kubang Kerian, Kelantan, Malaysia
[b] School of Chemical Sciences, Universiti Sains Malaysia, 11800 Penang, Malaysia

Received 13 May 2009; received in revised form 10 June 2009; accepted 13 August 2009
Available online 23 September 2009

Abstract

Structural defects in amorphous organo-modified silica nanoparticle have been studied via optical absorption and photoluminescence. The defect center, E′, oxygen defect center (ODCs), self-trapped exciton, OH-related surface defect, hydrogen-related species and carbon-related species were found in the amino-functionalized modified silica. These interesting emitting surface centers were observed in the range of vacuum ultraviolet (VUV), UV–vis and near-IR. Raman results were also demonstrated transverse- and longitudinal-optical pairs due to the surface defect-related optical properties.

Keywords: Amorphous silica; Nanoparticles; Co-condensation; Photoluminescence; Optical absorption

1. Introduction

Silica nanoparticles have been widely studied owing to several interesting optical phenomena caused by surface defects related to large surface/volume ratio [1]. This ratio provides the chemisorptions of OH groups on the surface of the particle and physisorption of water molecules. Removal of physisorped water (dehydration) and dehydroxylation of adjacent hydroxyl group by heat treatment activate particle surface towards structural defect. Point defects are generated from any defect in perfect SiO_4 continuous network, including oxygen and silicon vacancies. In the presence of organosilanes, silica particle may deal with a series of surface structural defects during condensation and/or cross-condensation reaction of organosilanes on the silica surface [2]. Numerous typical defects for silica nanoparticles such as surface E′ centers (paramagnetic positively charged oxygen vacancies, ≡Si•Si≡, or neutral dangling Si bonds, ≡Si•), non-bridging oxygen hole centers (NBOHCs; dangling oxygen bonds, ≡Si–O•), neutral oxygen deficient centers (ODCs; ≡Si–Si≡), twofold-coordinated silicon lone pair centers (≡Si–O–Si–O–Si≡), silanone group (O=Si=O), dioxasilyrane (=SiO_2), silylene (diamagnetic defect; =Si:) centers, peroxy linkage (PORs; ≡Si–O–O•), hydrogen-related species (≡Si–H and ≡Si–OH) and interstitial O_2 molecules [3–6]. These point defects can also be divided into two groups: paramagnetic and diamagnetic. Paramagnetic defects have optical absorption which represents half-occupied energy level in the optical band gap. Thus, hole transition or electron transition to the valence band is possible. Diamagnetic defects have absorption band associated with electron transition to the conduction band [7]. These defects and their combination are able to exhibit diversity of absorption and PL bands in broad range of wavelength, near-infrared, visible, and ultraviolet (UV). Hence, optical absorption and photoluminescence (PL) are the two useful properties for monitoring optical changes resulting from structural defect in the nanoparticle bulk and surface.

Since, silica nanoparticles have been extensively used as filler in fabrication of nanocomposites, modification of silica surface with coupling agent enhanced compatibility of filler with polymeric matrix. Co-condensation is one of the common modification techniques due to the homogeneous incorporation of organic functional group to the interior and exterior of the bulk of silica particle, compared with post-grafting method [8]. Although numerous co-condensation modification methods have been reported for porous silica, the modification of silica

* Corresponding author. Fax: +60 9 764 2026.
E-mail address: arismail@usm.my (I.A. Rahman).

0272-8842/$36.00
doi:10.1016/j.ceramint.2009.09.010

nanoparticles was less investigated. In our previous work [9], we have reported the preparation of organo-modified silica nanoparticles using APTES as modifier. Organo-functionalized silica nanoparticles were prepared by reacting tetraethyoxyhosilane (TEOS) and γ-aminopropyltriethoxysilane (APTES) in ethanol with water. In this continuation work, we focused on the evaluation of structural and optical properties of organo-modified silica nanoparticles by using XRD, PL, UV–vis and Raman techniques.

2. Experimental

2.1. Procedure

A quantity of 0.45 mol L^{-1} of TEOS (99%, Fluka) and 0.12 mol L^{-1} of APTES (99%, Aldrich) were first dissolved in 30 mL of absolute ethanol (99.5%, Systerm) simultaneously under low frequency ultrasound (Bransonic, Model 5510, 42 kHz) for 10 min. Then, 1 mL of distilled water was dropped into the reaction media with the fixed feed rate to facilitate hydrolysis of TEOS in the ultrasonic bath for 3 h. Then, the gelled samples were centrifuged and washed with ethanol and distilled water (3× 7 min, 6000 rpm). Drying was carried out using freeze drying as a non-thermal dehydration process under vacuum for overnight in a freeze dryer (Labconco, Freezon 12). The samples were heated at low temperature 220 °C for 2 h.

2.2. Characterization

Photoluminescence (PL) and Raman measurements were performed using Jobin Yvon HR 800 UV spectrophotometer equipped with HeCd ultraviolet laser (KIMMON IK320 IR-F, λ = 325 nm, 20 mW) source for PL and Argon ion laser (Spectra physics 183-D42, λ = 524 nm, 20 mW) source for Raman at room temperature, respectively. Solid state UV–vis absorption spectra were collected using PerkinElmer Lamda 45 spectrophotometer. X-ray diffraction patterns were recorded using SIEMENS D5000 X-ray diffractometer.

3. Results and discussion

Organo-modified silica nanoparticles have been prepared through co-condensation method by using γ-aminopropyltriethoxysilane (APTES). Fig. 1 shows TEM of the powders. For comparison, a pure silica powder with particle size ∼10 nm was synthesized by using TEOS [10].

The organo-modified powder consists of nearly spherical with average particle size of ∼60 nm and low aggregation (Fig. 1(a)). This may be due to the presence of organic groups on the silica during surface modification. Under the base-catalyzed condition, the gel network is predominantly formed from $Si(OEt)_4$ because it reacts faster than $RSi(OEt)_3$ and then condenses to form incomplete three-dimensional gel network that might prevent from the formation of curvature of spherical particles. The particle size of modified silica is sixfold higher than that of the pure silica may be due to the increase in the concentration of $–NH_2$ group that leads to the enhancement in the rate of hydrolysis and condensation reaction, which consequently, induces the growth of the larger particles.

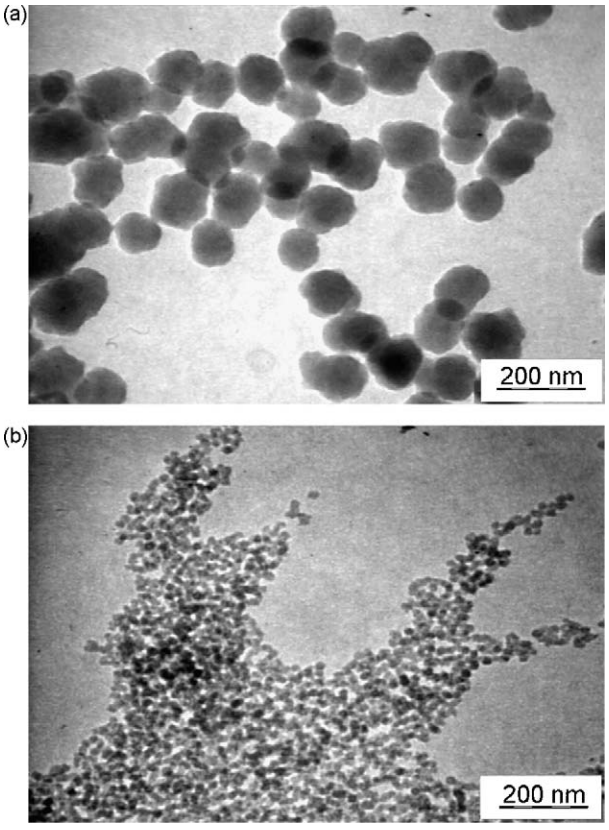

Fig. 1. TEM images of (a) modified silica, and (b) pure silica.

Fig. 2 shows the XRD patterns of an amorphous state of organic-modified and pure nanosilica produced using APTES and TEOS, respectively. The broad XRD reflection peaks may be due to the small size effect and incomplete inner structure of the particles [11]. The structural stability of silica does not change with the incorporation of organic group into silica.

Fig. 3 shows the PL spectra of organo-modified and pure silica at room temperature. Several emission bands were observed for organo-modified silica nanoparticles in the UV, blue, green, and IR spectral regions. The main emission band at ∼414 nm (blue band, ∼2.99 eV) is attributed to the neutral oxygen vacancies (ODCs; ≡Si–Si≡) and intrinsic diamagnetic defect center (two trapped center; ≡Si–O–Si–O–Si≡), self-trapped exciton (photoexcited electron–hole pairs; STE) that spatially confined with SiO_4 tetrahedron [12–14] and carbon-related species (resulting from organo-group in APTES) [15]. The blue light emitting center is corresponding to the defect resulting from the dehydroxylation reaction of a pair of geminal silanol group on the surface of silica by heat treatment. Thus, the intensity of blue light emission can be enhanced by increasing the concentration of silanol groups that may generate some defect points, such as silanone and silylene from dehydroxylation process in appropriate heat treatment. In addition, some disorderly and defect center can be expected by introducing an organosilane derivative to nanometer-size amorphous silica particles through a linkage between two

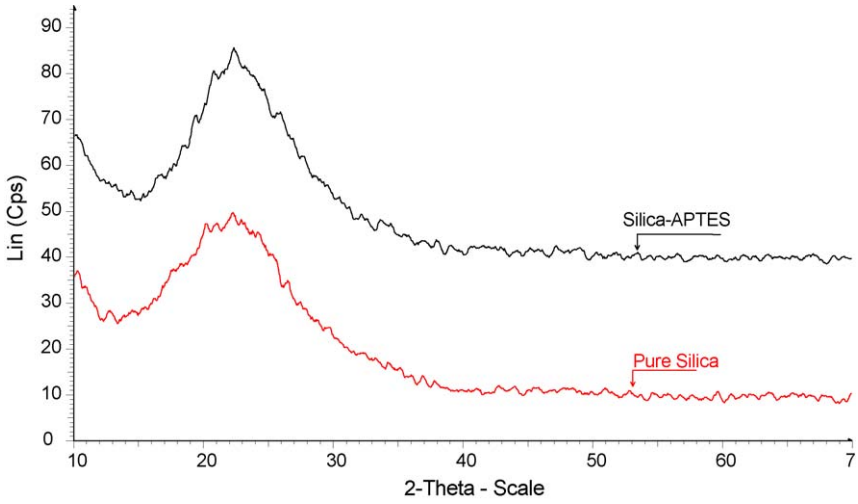

Fig. 2. XRD patterns of organo-modified and pure silica nanoparticles.

different types of molecules (TEOS and APTES as precursors) in co-condensation method. Therefore, an enhancement in PL emission band is due to the presence of APTES modifier. A significant increase in the intensity of the blue band might be due to an increasing oxygen vacancy center on the surface and within the particles in modified silica in comparison with that in pure silica. In other words, different kinetic behaviours in hydrolysis and condensation reaction between TEOS and APTES and also the possibility of occurring cross-condensation reactions among them (under co-condensation procedure) [9] can be a key factor in the generation of some structural defects in the modified silica (two different precursors) as compared to the pure silica (single precursor). The modified silica blue band has been shifted towards the higher energy range (blue shift, ~13 nm) in comparison with that of pure silica (~427 nm, ~2.9 eV). This is possibly due to the difference in sample preparation parameter (normal sol–gel *vs.* co-condensation), leading to the different structural defects (different defect concentrations, e.g. oxygen deficiency) in the final product.

The intense peak at ~514 nm (green band, ~2.4 eV) is assigned to the presence of hydrogen-related species (≡Si–H) [11]. Glinka et al. [16] stated that the green emission is related to the bending vibration of (≡Si–H) bond on the silica surface. This vibronic coupling is depended on the temperature and the local geometry of complexes [17]. The broader PL feature in modified silica is indicated a broad distribution of the energy levels associated with the relevant emission centers [18]. Near-UV luminescence bands at ~359 (~3.4 eV) and ~341 (~3.6 eV) nm are associated to the different kinds of interacting silanol species (OH-related species) with adsorbed molecular water on the surface and within the particles [19]. Luminescence center at ~3.6 eV may be related to Si–O–C species (carbon-related species) formed by defects and carbon atom during the thermal treatment [15]. These bands reveal high intense emission in modified silica as compared to that in pure silica. The weak IR absorption bands at ~682 (~1.8 eV) and ~718 (~1.7 eV) nm and a broad band at around ~800 (~1.54 eV) nm (red band) attributed to the non-bridging oxygen hole center (NBOHC; ≡Si–O$^{\bullet}$) generated from hydroxyl defect at bulk and surface, respectively [12,20,21]. NBOHC resulted from the fission of strained Si–O–Si bond under heat treatment.

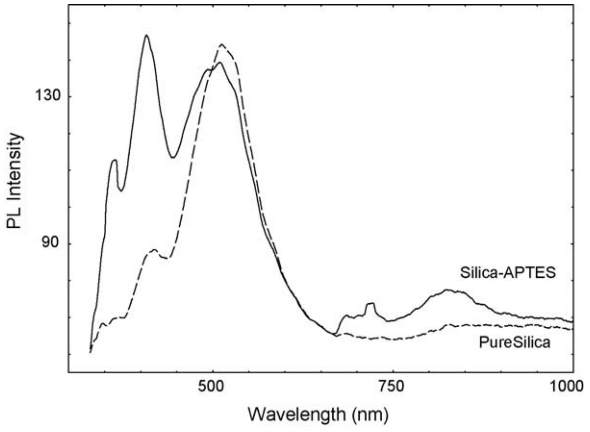

Fig. 3. Room temperature PL spectra of modified silica (solid-line) and pure silica (dash-line) nanoparticles.

$$\equiv Si-O-Si\equiv \rightarrow \equiv Si-O^{\bullet} + {}^{\bullet}Si\equiv$$

NBOHC defect is not found in pure silica. There is an energetic difference between bulk and surface NBOHCs resulting from an incorporation of non-bridging oxygen atoms into undistorted SiO_4 tetrahedrons (bulk species) and into distorted tetrahedrons creating twofold Si–O rings (surface species) [17]. Thus, the luminescence activities in modified silica were enhanced due to hybrid polymeric silica chain (TEOS–APTES) under co-condensation reaction that led to the increase in structural defect on the surface of particles.

Fig. 4(a) demonstrates the optical absorption of modified and pure silica in the UV region. Three main absorption bands were observed at ~461 (~2.7 eV), ~306 (~4 eV) and ~243 (~5 eV) nm. The band at ~2.7 eV is generated from neutral oxygen vacancies (ODCs) defect. This peak has not been found in pure silica. A peak at ~4 eV is attributed to the non-bridging oxygen hole center [7]. The absorption band observed near to

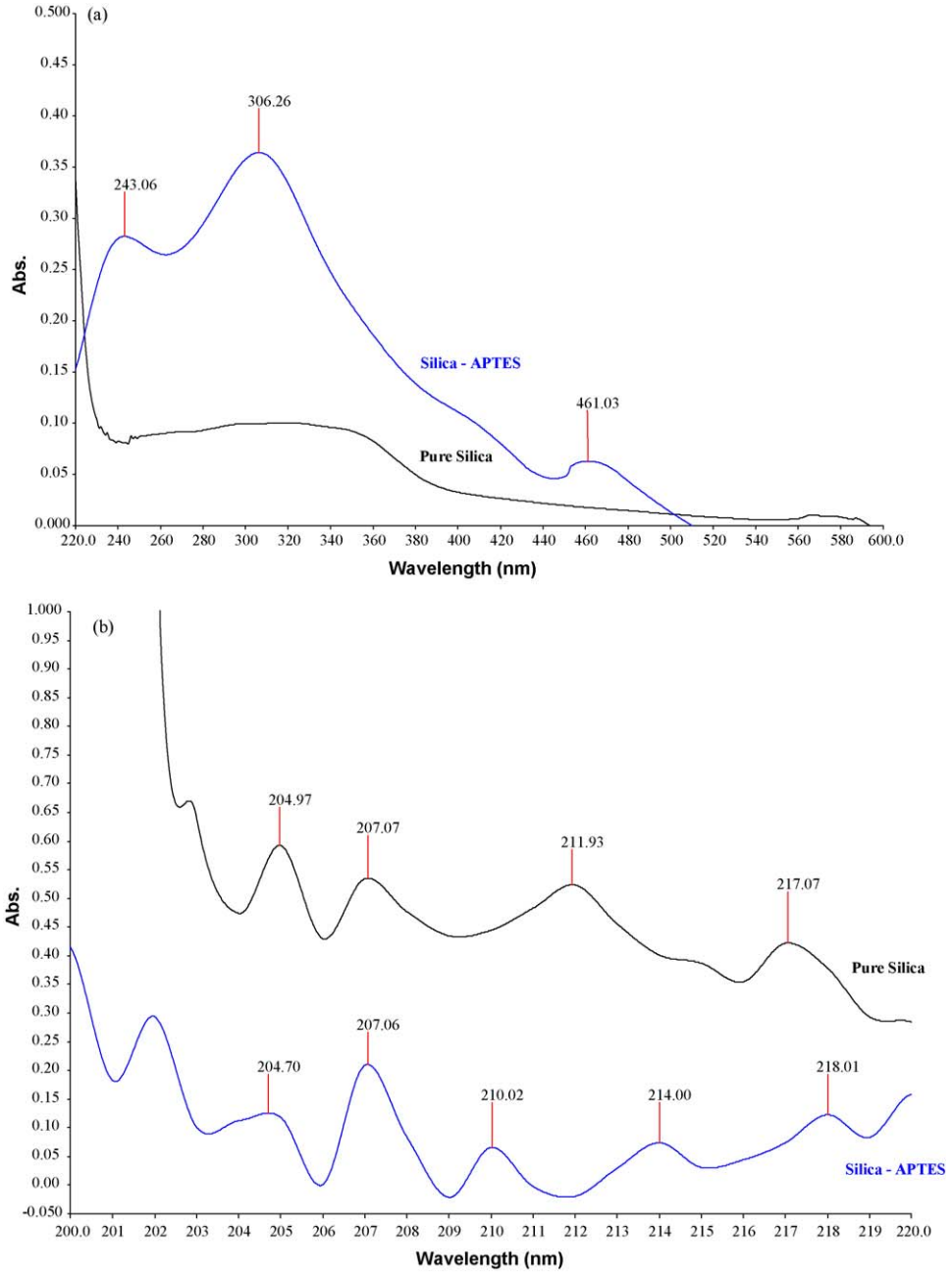

Fig. 4. Optical absorptions of modified silica and pure silica in (a) UV range, and (b) near vacuum UV region.

~5 eV is corresponding to the B_2-center [22,23]. Pure silica was UV-inactive at ~5 eV. This band is denoted as a neutral (diamagnetic) oxygen vacancy that comprises a simple oxygen vacancy (≡Si–Si≡) and twofold-coordinated silicon (–O–$Si^{\bullet}$–O–). Theoretical studies using *ab initio* molecular orbital calculation showed that non-paramagnetic defect (≡Si–Si≡) is caused by a singlet–singlet transition [24]. The absorption shoulder at ~415 nm (~3 eV) that might be attributed to the defect point in dicoordinated silicon lone pair (≡Si–O–Si–O–Si≡) [7]. Our finding shows a good agreement with the results reported in literatures [7,22–24]. However, a slight difference in the peak position may be related to the manufacturing process, thermal treatment and excitation energy.

Fig. 4(b) shows the optical absorption of modified and pure silica near vacuum ultraviolet (VUV) region. Optical band at ~218 nm (~5.6 eV) is related to the surface center (≡Si–$O)_2$Si=O (silanone group) [25]. This peak has not been observed for pure silica. Peaks at ~210 (~5.9 eV) and ~207 (~5.98) nm are associated to the E′ center as an intrinsic interior defect [26]. The most accepted model of E′ is oxygen deficiency related center (≡$Si^{\bullet}$Si≡) [27]. These defects are generated from the displacement of oxygen from a perfect Si–O–Si network that have trapped hole. Absorption band at ~204 (~6 eV) and ~201 (~6.1 eV) nm is correlated to the E′ center in surface (≡$Si^{\bullet}$) [7].

Fig. 5 shows conventional room temperature Raman spectra of silica and modified silica in a wavelength range of 4050–

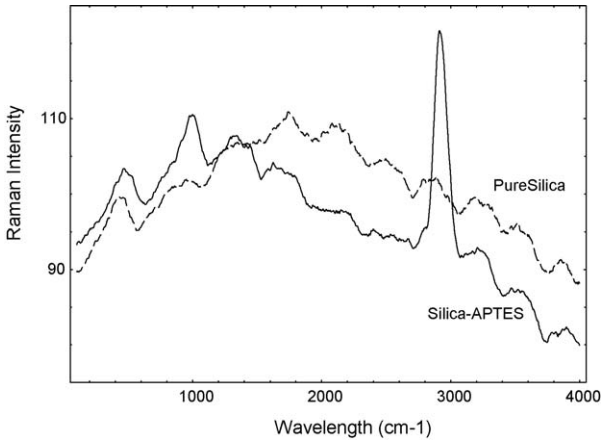

Fig. 5. Raman spectra of modified silica (solid-line), and pure silica (dash-line) nanoparticles.

50 cm^{-1}. Bands at ~440 (ν1 bending mode), ~800 (ν3 stretching mode), ~1040 (ν4 stretching mode), and ~1200 (ν4 stretching mode) cm^{-1} are attributed to the Raman activity of siloxane bond (Si–O–Si) in intrinsic silica structure [28]. Peaks at higher energy, 4000–3000 cm^{-1}, display a variety of Si–OH species on the silica surface. They are correlated to the stretching vibration in the isolated silanol groups [29] and interaction between surface silanol with adsorbed molecular water through a weak and strong hydrogen bond [30]. Significantly, high intense peak at ~950 cm^{-1} is indicated to the presence of organic groups (C–H stretching mode) on the surface that was only appeared for the modified silica [31]. Interestingly, the peaks at ~1060 and ~1200 cm^{-1} are related to the presence of transverse-optical (TO) and longitudinal-optical (LO) pairs, respectively [32,33]. The symmetric stretching bands at ~490 (D_1) and ~610 (D_2) cm^{-1} have been ascribed to the bulk [34] and internal surface [35] defects in fourfold and threefold ring of SiO_2 tetrahedral structure, respectively. Consequently, Raman studies have been confirmed the surface-related optical properties in silica nanoparticles in both modified and pure forms.

4. Conclusion

The amorphous organo-modified silica nanoparticles have shown some interesting optical and luminescence activities in a wide range of wavelength from vacuum ultraviolet to infra-red. The results showed the presence of both diamagnetic (trapped electron center) and paramagnetic (trapped hole-center) defects in the bulk and surface of the particles. The PL optical activity in modified silica has shown a broad range from near VUV to near IR (including blue, green, and red optical band). In contrast, pure silica showed a narrower range of optical activity (only blue and green band) and no red optical band was observed as well. The result also displayed more intense blue band that related to the higher defect density, in modified silica than that in silica. The existence of bulk and surface-related optical activities in Raman is another intriguing finding for developing the light emitting devices. Thus, organo-modified silica nanoparticles can be a potential candidate with remarkable optical properties for application as optoelectronic devices.

Acknowledgements

The authors are thankful to the Ministry of Higher Education for financial support of this research via Grant No. FRGS-203/PKIMIA/671174. M. Jafarzadeh wishes to thank the Universiti Sains Malaysia (USM) for USM-Fellowship.

References

[1] A. Anedda, C.M. Carbonaro, F. Clemente, R. Corpino, P.C. Ricci, Low temperature investigation of the blue emission in mesoporous silica, Mater. Sci. Eng. C 25 (2005) 631–634.
[2] I. Hernández, G. Córdoba, J. Padilla, J. Méndez-Vivar, R. Arroyo, Photoluminescence properties of silica monoliths codoped with terbium and germanium, Mater. Lett. 62 (2008) 1945–1948.
[3] T. Mohanty, N.C. Mishra, S.V. Bhat, P.K. Basu, D. Kanjilal, Dense electronic excitation induced defects in fused silica, J. Phys. D: Appl. Phys. 36 (2003) 3151–3155.
[4] N. Kurumoto, T. Yamada, T. Uchino, Enhanced blue photoluminescence from $SiCl_4$-treated nanometer-sized silica particles, J. Non-Cryst. Solid 353 (2007) 684–686.
[5] L. Skuja, B. Güttler, D. Schiel, A.R. Silin, Infrared photoluminescence of preexisting or irradiation-induced interstitial oxygen molecules in glassy SiO_2 and a-quartz, Phys. Rev. B 58 (1998) 14296–14304.
[6] M.C. Neves, T. Trindade, M. Pares, J. Wang, M.J. Soares, A. Neves, T. Monteiro, Photoluminescence of zinc oxide supported on submicron silica particles, Mater. Sci. Eng. C 25 (2005) 654–657.
[7] L. Skuja, Optically active oxygen-deficiency-related centers in amorphous silicon dioxide, J. Non-Cryst. Solid 239 (1998) 16–48.
[8] T.M. Suzuki, T. Nakamura, K. Fukumoto, M. Yamamoto, Y. Akimoto, K. Yano, Direct synthesis of amino-functionalized monodispersed mesoporous silica spheres and their catalytic activity for nitroaldol condensation, J. Mol. Catal. A 280 (2008) 224–232.
[9] I.A. Rahman, M. Jafarzadeh, C.S. Sipaut, Synthesis of organo-functionalized nanosilica via a co-condensation modification using γ-aminopropyltriethoxysilane (APTES), Ceram. Int. 35 (2009) 1883–1888.
[10] M. Jafarzadeh, I.A. Rahman, C.S. Sipaut, Synthesis of silica nanoparticles by modified sol–gel process: the effect of mixing modes of the reactants and drying techniques, J. Sol–Gel Sci. Technol. 50 (2009) 328–336.
[11] Z. Wei, P. Yan, W. Feng, J. Dai, Q. Wang, T. Xia, Microstructural characterization of Ni nanoparticles prepared by anodic arc plasma, Mater. Charac. 57 (2006) 176–181.
[12] Y.D. Glinka, S.-H. Lin, Y.-T. Chen, Two-photon-excited luminescence and defect formation in SiO_2 nanoparticles induced by 6.4-eV ArF laser light, Phys. Rev. B 62 (2000) 4733–4743.
[13] H. Yang, X. Yao, D. Huang, Sol–gel synthesis and photoluminescence of AlP nanocrystals embedded in silica glasses, Opt. Mater. 29 (2007) 747–752.
[14] C. Itoh, K. Tanimura, N. Itoh, Optical studies of self-trapped excitons in SiO_2, J. Phys. C: Solid State Phys. 21 (1988) 4693–4702.
[15] H. He, Y. Wang, H. Tang, Intense ultraviolet and green photoluminescence from sol–gel derived silica containing hydrogenated carbon, J. Phys. Condens. Mater. 14 (2002) 11867–11874.
[16] Y.D. Glinka, S.-H. Lim, Y.-T. Chen, The photoluminescence from hydrogen-related species in composites of SiO_2 nanoparticles, Appl. Phys. Lett. 75 (1999) 778–780.
[17] Y.D. Glinka, S.-H. Lin, Y.-T. Chen, Time-resolved photoluminescence study of silica nanoparticles as compared to bulk type-III fused silica, Phys. Rev. B 66 (2002) 354041–3540410.
[18] T. Yamada, M. Nakajima, T. Suemoto, T. Uchino, Formation and photoluminescence characterization of transparent silica glass prepared by solid-phase reaction of nanometer-sized silica particles, J. Phys. Chem. C 111 (2007) 12973–12979.

[19] C.M. Carbonaro, D. Chiriu, R. Corpino, P.C. Ricci, A. Anedda, Photoluminescence characterization of sol–gel prepared low density silica samples, J. Non-Cryst. Solid 353 (2007) 550–554.
[20] Y. Sakurai, Photoluminescence of oxygen-deficient-type defects in γ-irradiated silica glass, J. Non-Cryst. Solid 352 (2006) 5391–5398.
[21] Y. Yang, B.K. Tay, X.W. Sun, H.M. Fan, Z.X. Shen, Photoluminescence and growth mechanism of amorphous silica nanowires by vapor phase transport, Physica E 31 (2006) 218–223.
[22] L.N. Skuja, A.N. Streletsky, A.B. Pakovich, A new intrinsic defect in amorphous SiO_2: twofold coordinated silicon, Solid State Commun. 50 (1984) 1069–1072.
[23] R. Tohmon, H. Mizuno, Y. Ohki, K. Sasagane, K. Nagasawa, Y. Hama, Correlation of the 5.0- and 7.6-eV absorption bands in SiO_2 with oxygen vacancy, Phys. Rev. B 39 (1989) 1337–1345.
[24] D.L. Griscom, Optical properties and structure of defects in silica glass, J. Ceram. Soc. Jpn. 99 (1991) 923–942.
[25] V.A. Radtsig, I.N. Senchenya, Hydrogenation of the silanone groups $(\equiv Si–O)_2Si{=}O^{\bullet}$. Experimental and quantum-chemical studies, Russ. Chem. Bull. 45 (1996) 1849–1856.
[26] T.E. Tsai, D.L. Griscom, E.J. Friebele, Mechanism of intrinsic Si E′-center photogeneration in high-purity silica, Phys. Rev. Lett. 61 (1988) 444–446.
[27] G. Pacchioni, G. Ieranò, A.M. Márquez, Optical absorption and nonradiative decay mechanism of E' center in silica, Phys. Rev. Lett. 81 (1998) 377–380.
[28] P. Umari, A. Pasquarello, First-principles analysis of the Raman spectrum of vitreous silica: comparison with the vibrational density of states, J. Phys. Condens. Mater. 15 (2003) S1547–S1552.
[29] A. Anedda, C.M. Carbonaro, F. Clemente, L. Corda, R. Corpino, P.C. Ricci, Raman investigation of surface OH-species in porous silica, J. Phys. Chem. B 107 (2003) 13661–13664.
[30] A. Anedda, C.M. Carbonaro, F. Clemente, L. Corda, R. Corpino, P.C. Ricci, Surface hydroxyls in porous silica: a Raman spectroscopy study, Mater. Sci. Eng. C 23 (2003) 1069–1072.
[31] P.K. Sekhar, N.S. Ramgir, S. Bhansali, Metal-decorated silica nanowires: an active surface-enhanced Raman substrate for cancer biomarker detection, J. Phys. Chem. C 112 (2008) 1729–1734.
[32] N. Chiodini, F. Meinardi, F. Morazzoni, A. Paleari, R. Scotti, G. Spinolo, Tin doped silica by sol–gel method: doping effects on the SiO_2 Raman spectrum, Solid State Commun. 109 (1999) 145–150.
[33] Y.D. Glinka, M. Jaroniee, Shape-selective Raman scattering from surface phonon modes in aggregates of amorphous SiO_2 nanoparticles, J. Appl. Phys. 82 (1997) 3499–3507.
[34] F.L. Galeener, Planar rings in vitreous silica, J. Non-Cryst. Solids 49 (1982) 53–62.
[35] J.C. Phillips, Structural model of Raman "defect" bands of vitreous silica, Phys. Rev. B 35 (1987) 6409–6413.